Arch. Metall. Mater. **70** (2025), 2, 879-882

DOI: https://doi.org/10.24425/amm.2025.153489

A. AHMED[1*], K. MATSUDA[2*], S. LEE[2], T. TSUCHIYA[2], K. NISHIMURA[2], N. NUMOMURA[2], H. TODA[3], K. HIRAYAMA[4], K. SHIMIZU[5], M. YAMAGUCHI[6], T. TSURU[7]

CHARACTERIZATION OF THE T'-PHASE INTERFACE IN Al-Zn-Mg ALLOY ALONG THE <112> ZONE DIRECTION OF Al-MATRIX

In this study, we observed the T'-phase for the first time along the <112> zone axis of the Al matrix. The orientation relationship, shape, misfit value, and interfacial conditions between the T'-phase and the Al matrix were investigated using high-resolution transmission electron microscopy (HR-TEM). The T'-phase exhibited a fine cubic morphology, and we clarified each facet by analyzing diffraction patterns and fast Fourier transform (FFT) images. Additionally, we identified the $(1\bar{1}1)_{Al}//(001)_{T'}$, $(1\bar{1}0)_{Al}//(\bar{1}00)_{T'}$ interface between the T'-phase and the Al matrix along the $[1\bar{1}\bar{2}]_{Al}//[010]_{T'}$ zone direction.

Keywords: HRTEM; $Mg_{32}(Al,Zn)_{49}$; precipitation; T'-phase; AlZnMg; orientation relationship

Abbreviation

TEM: Transmission Electron Microscopy; HRTEM: High Resolution Transmission Electron Microscopy; IFFT: Inverse Fast Fourier Transform; FFT: Fast Fourier Transform; SAED: Selected Area Electron Diffraction.

1. Introduction

Wrought aluminum (Al) alloys are commonly used for radial compressor impellers in vehicle turbochargers due to their relatively high specific strength, which results in low inertia for the compressor wheel [1,2]. Previous research has explored various combinations of Zn and Mg additions. Based on the phase diagram, a high Zn/Mg ratio promotes the formation of the η phase, a balanced ratio leads to the coexistence of both T and η phases, and a low Zn/Mg ratio predominantly produces the T phase. In this study, a low Zn/Mg ratio was used. Earlier studies have shown that the η phase is the primary strengthening precipitate in 7xxx alloys with higher Zn/Mg ratios, while the T phase is more prevalent in alloys with lower Zn/Mg ratios [3-5]. The precipitation sequence of the T-phase is reported as follows [6,7]:

SSSS → GP-zone → T''-phase(metastable) →
T'-phase (metastable) → T-phase (equilibrium)

The T' phase is often overlooked by researchers because it rarely appears as a strengthening phase in 7xxx series alloys and typically forms at high aging temperatures above 200°C [8,9] or under severely overaged conditions [10]. However, Yang [11] recently reported an Al-Zn-Mg alloy strengthened by T-type phases, which demonstrated superior strength and corrosion resistance compared to alloy 7150, which is hardened by η-type phases. Additionally, a novel heat-resistant Al-Zn-Mg alloy [9] was reported to achieve a high yield strength of approximately 200 MPa at 200°C, attributed to numerous fine metastable T phases formed within the grain interiors. This suggests that T-type phases hold great potential for applications requiring enhanced corrosion resistance and thermal stability [9,11].

[1] UNIVERSITY OF TOYAMA, GRADUATE SCHOOL OF SCIENCE AND ENGINEERING FOR EDUCATION, TOYAMA, 930-8555, JAPAN
[2] UNIVERSITY OF TOYAMA, GRADUATE SCHOOL OF SCIENCE AND ENGINEERING FOR RESEARCH, TOYAMA, 930-8555, JAPAN
[3] KYUSHU UNIVERSITY, DEPARTMENT OF MECHANICAL ENGINEERING, FUKUOKA, 819-0395, JAPAN
[4] KYOTO UNIVERSITY, DEPARTMENT OF MATERIALS SCIENCE AND ENGINEERING, KYOTO, 606-8501, JAPAN
[5] TOTTORI UNIVERSITY, GRADUATE SCHOOL OF SCIENCE AND ENGINEERING, 4-101 KYOAMA MINAMI, TOTTORI, JAPAN
[6] CENTER FOR COMPUTATIONAL SCIENCE AND E-SYSTEMS, JAPAN ATOMIC ENERGY AGENCY, TOKAI, IBARAKI, 319-1195, JAPAN
[7] NUCLEAR SCIENCE AND ENGINEERING CENTER, JAPAN ATOMIC ENERGY AGENCY, TOKAI, IBARAKI, 319-1195, JAPAN

* Corresponding authors: abrar.kfc@gmail.com, matsuda@sus.u-toyama.ac.jp

The shape of precipitates is crucial in determining the misfit and interface with the matrix [12]. The interface between the precipitate and the matrix plays a significant role in influencing mechanical properties [13,14]. In other alloy systems, the interface is often modified to enhance the material's strength [15,16]. Moreover, understanding the interface is essential for analyzing hydrogen trapping, which can lead to crack initiation and embrittlement of the material [17].

This study focuses on the T'-phase along the <112> zone axis of the Al matrix using transmission electron microscopy (TEM). We observed the fine cubic morphology of the T'-phase and clarified each facet by analyzing diffraction patterns and fast Fourier transform (FFT) images. Additionally, we examined the interface between the T'-phase and the Al matrix using high-resolution TEM images.

2. Experimental procedure

In this experiment, 99.99% aluminum, 99.9% zinc, and 99.9% magnesium ingots were used to produce the alloy, which was smelted at 720°C in an electric resistance furnace. Zinc and magnesium were added simultaneously, and the mixture was stirred thoroughly before degassing, refining, and casting in a metal mold at 400°C. The resulting alloy, designated ZM14, had a composition of Al-1.1 at.% Zn-4.3 at.% Mg with a Zn/Mg ratio of 0.255. After homogenization at 748 K for 86.4 ks, the ingots were hot-rolled to 10 mm and cold-rolled to 2.0 mm before solution heat treatment and aging. Samples for microstructure observation were cold-rolled to 0.2 mm, mechanically polished, and prepared for TEM observation through twin-jet polishing. TEM analysis was conducted using a Topcon EM-002B at 120 kV.

3. Results and discussion

To elucidate the microstructure of the ZM14 alloy aged at 473 K for 2000 minutes, the conditions are shown in Fig. 1. The TEM bright-field image displays the precipitates within the α-Al matrix of the sample aged at 200°C for 2000 minutes (Fig. 1(a)). The selected area electron diffraction (SAED) pattern (Fig. 1(b)) indicates that the incident beam direction is along the <112> axis of the α-Al matrix. The diffraction spots from the precipitates, indicated by red arrows, suggest the presence of a metastable T" (T') phase and a stable T-phase. The orientation relationships between the matrix and the T", T', and T phases are the same [20,21]. More recently, it was reported that the T"-phase is coherent, the T'-phase is semi-coherent, and the T-phase is incoherent [6]. Understanding the microstructure of these phases in low magnification images is complicated that the habit plane of the T-phase is {111} in the Al matrix, which includes four distinct directions ([010], [312], [3$\bar{1}$2], and [310]) [22]. Along the <112> zone direction of the Al matrix, the corresponding diffraction pattern shows the 2/5 and 3/5 diffraction spots of the precipitate between 000_{Al} and 220_{Al}, identifying the T-phase morphology in the matrix [21], as shown in Fig. 1(b).

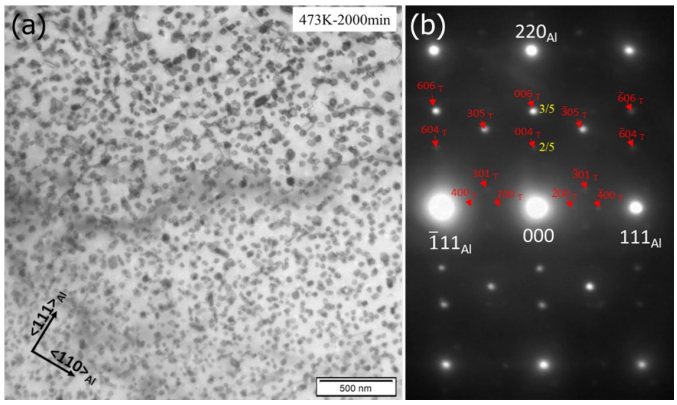

Fig. 1. (a) TEM bright-field image in ZM14 alloy after aging at 473K for 2000 min. (b) corresponding selected area diffraction pattern along <112>Al zone direction, red arrow shows the T(T', T") phase diffraction spots

Along the [$\bar{1}\bar{1}$2] zone direction of the Al matrix, which is parallel to the [010] zone direction of the T' phase [21] (Fig. 2),

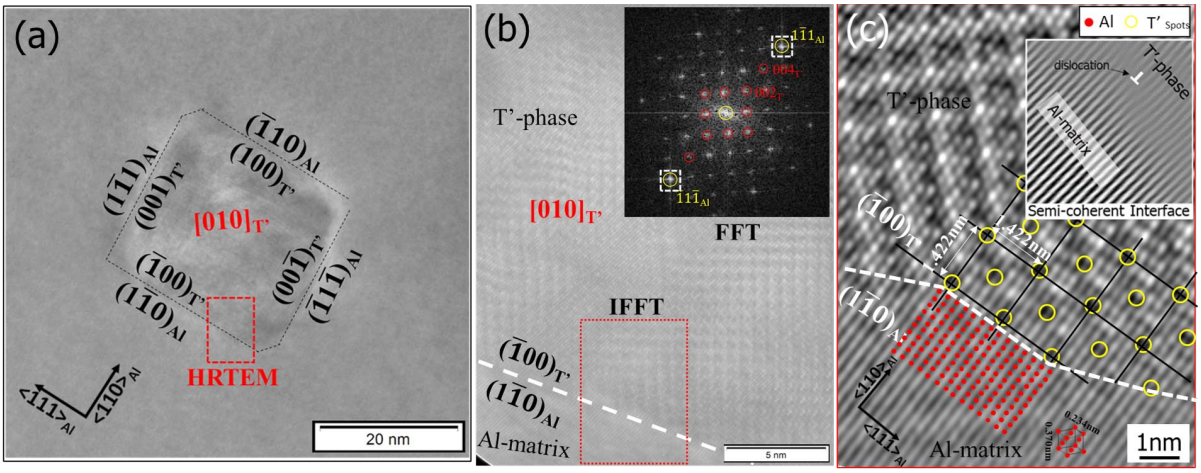

Fig. 2. (a) Magnified TEM bright-field image <112> in ZM14 alloy after aging at 473K for 2000 min, (b) HRTEM image of the T' interface taken by the red dotted rectangle area in (a), (c) inverse FFT image taken by the red dotted rectangle area in (a) is $[11\bar{2}]_{Al}$ // [010]T' || $(1\bar{1}0)_{Al}$ // $(\bar{1}00)$T'

the morphology of the precipitate exhibits a complete cubic shape. Two facets of the T'-phase align with the {111} facets of the Al matrix. The planes $(1\bar{1}1)_{Al}//(001)_{T'}$ and $(1\bar{1}0)_{Al}//(\bar{1}00)_{T'}$ are parallel (Fig. 2(a)). The high-resolution transmission electron microscopy (HRTEM) image (Fig. 2(b)), taken from the $(1\bar{1}0)_{Al}//(\bar{1}00)_{T'}$ facet, highlights the red rectangle area in Fig. 2(a).

The FFT image obtained from the red rectangle area (Fig. 2(b)) shows that the diffraction spot of $1\bar{1}1_{Al}$ is parallel to $001_{T'}$, as illustrated in Fig. 2(b). The IFFT image clearly indicates $[\bar{1}\,\bar{1}\,2]_{Al}//[010]_{T'}$ and $(1\bar{1}0)_{Al}//(\bar{1}00)_{T'}$, as shown in Fig. 2(c). The Al matrix spot along the $[\bar{1}\,\bar{1}\,2]$ zone direction is denoted by the red closed circle, while the dark T' lattice spots along the [010] zone direction are marked by the yellow open circles (Fig. 2(c)). The d-spacing between the dark spots in the precipitate area identifies the lattice spacing of the T' phase as 1.422 nm. The interface between the T' phase and the Al matrix is semi-coherent [6], as determined by selecting the 111_{Al} diffraction spots in the FFT image (Fig. 2(b)), as illustrated in Fig. 2(c). A previous report has identified the lattice parameter of 1.422 nm as corresponding to the T-phase [23]. The orientation of the T' phase with respect to the Al matrix is:

$$[\bar{1}\,\bar{1}\,2]_{Al}//[010]_{T'}$$
$$(1\bar{1}1)_{Al}//(001)_{T'}\ [21],$$
$$(1\bar{1}0)_{Al}//(\bar{1}00)_{T'}$$

Fig. 3 shows the schematic orientation relationship between the T'-phase and the Al matrix. Fig. 3(a) presents a 3D schematic model of the T'-phase and the Al matrix, while Fig. 3(b) illustrates a 2D model that depicts the same orientation observed in Fig. 2(a). We calculated the misfit between T'-phase and Al-matrix. By using the Eq. (1) [24].

$$\delta(\%) = \frac{\left| m \times d\{h_2k_2l_2\}_p - n \times d\{h_1k_1l_1\}_{Al} \right|}{n \times d\{h_1k_1l_1\}_{Al}} \qquad (1)$$

Here, $\delta(\%)$ represents the misfit value, m and n are integer multiples of the lattice constant, $d\{h_2k_2l_2\}_p$ lattice constant of the precipitate phase, and $d\{h_1k_1l_1\}_{Al}$ lattice constant of the matrix phase. The misfit between the T'-phase and the Al matrix is 1.26%, with n = 6 ($6 \times d_{\{111\}Al} = 0.234$ nm) and m = 1 ($1 \times d_{\{100\}T'} = 1.422$ nm). According to previous research, hydrogen atoms do not trap within the crystal structure of the β-phase [16]. However, there is a possibility of trapping at the semi-coherent interface due to mismatched intervals [23], which leads to hydrogen trapping at the interface.

4. Conclusions

This study successfully elucidated the microstructural characteristics of the ZM14 alloy, specifically focusing on the T'-phase and its orientation relationship with the Al matrix. High-resolution transmission electron microscopy (HRTEM) revealed that the T'-phase exhibits a complete cubic morphology aligned along the $[\bar{1}\,\bar{1}\,2]$ zone direction of the Al matrix, demonstrating the precise orientation relationships with the Al matrix facets. These findings contribute to the understanding of the effects of microstructural evolution on the alloy's mechanical properties and hydrogen trapping behavior, paving the way for the design of advanced aluminum alloys with improved performance characteristics.

Acknowledgment

This work was supported by Japan Science and Technology Agency CREST (Grant No. JPMJCR1995) and Japan Society for the Promotion of Science KAKENHI (Grant Nos. 20H02479, 22500173). A part of this work was also supported by the University of Toyama's Advanced Aluminum International Research Center and the President's Discretionary Funds of FY2022 and FY2023. The authors thank the Otsuka Toshimi Scholarship Foundation for their financial support (Ref. # 24-6) to A. Ahmed.

The results were presented during 14th Polish Japanese Joint Seminar on Micro and Nano Analysis (3-6.09.2024, Toyama, Japan).

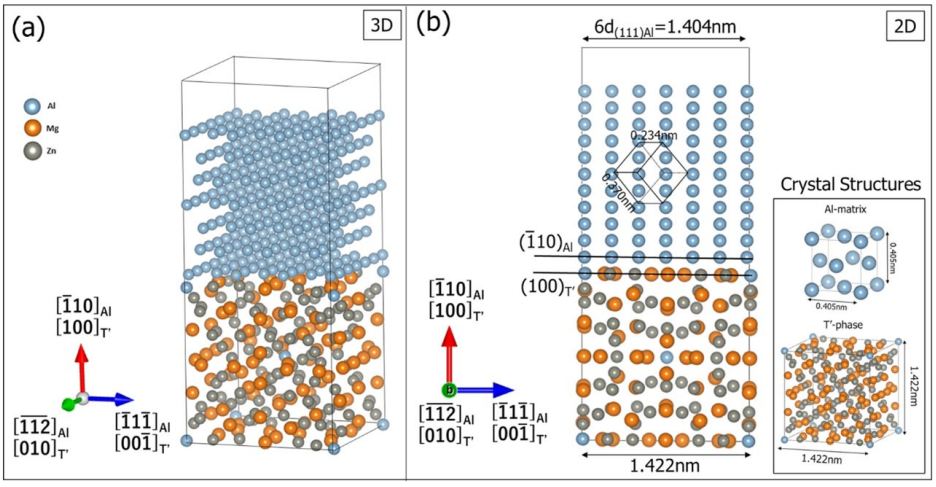

Fig. 3. Schematic model and detailed orientation relation between T'-phase and Al-matrix according to the Fig. 2(a)

REFERENCES

[1] G. Wallace, A. Jackson, S. Midison, Novel Method for Casting High Quality Aluminum Turbocharger Impellers. SAE Int. J. Mater. Manuf. **3** (1), 405-412, (2010).
DOI: https://doi.org/10.4271/2010-01-0655

[2] A.P. Jackson, G.R. Wallace, S.P. Midson, Adv. Mater. Proc. Apr. 19-22 (2010).

[3] R.S. Danchik, Nonferrous Metallurgy-I. Light Metals: Aluminium, Beryllium, Titanium, and Magnesium. Analytical Chemistry **45**, 5 113-128 (1973):

[4] A. Abrar, S. Lee, T. Tsuchiya, K. Matsuda, Microstructure observation of Al-Zn-Mg alloy with high Mg content. Solid State Phenomena **353**, Trans. Tech. Publication, Ltd., 5 Dec. 2023, pp. 73-77.

[5] H. Liang, S.-L. Chen, Y.A. Chang, A Thermodynamic Description of the Al-Mg-Zn System. Metallurgical and Materials Transactions A **28**A, 1725, september (1997).

[6] S. Hou, P. Liu, D. Zhang, J. Zhang, L. Zhuang, Precipitation hardening behavior and microstructure evolution of Al-5.1 Mg-0.15Cu alloy with 3.0Zn (wt.%) addition. J. Mater. Sci. **53** (5), 3846-3861 (2018). DOI: https://doi.org/10.1007/s10853-017-1811-1

[7] L. Stemper, B. Mitas, T. Kremmer, S. Otterbach, P.J. Uggowitzer, et al., Age-hardening of high pressure die casting AlMg alloys with Zn and combined Zn and Cu additions. Materials & Design **181**, 107927 (2019).
DOI: https://doi.org/10.1016/j.matdes.2019.107927

[8] N. Afify, A.-F. Gaber, G. Abbady, Fine scale precipitates in Al-Mg-Zn alloys after various aging temperatures. Mater. Sci. Appl. **02** (05), 427-434 (2011).
DOI: https://doi.org/10.4236/msa.2011.25056

[9] N. Takata, M. Ishihara, A. Suzuki, M. Kobashi, Microstructure and strength of a novel heat-resistant aluminum alloy strengthened by T-Al6Mg11Zn11 phase at elevated temperatures. Mater. Sci. Eng. A **739**, 62-70 (2019).
DOI: https://doi.org/10.1016/j.msea.2018.10.034

[10] S.K. Maloney, K. Hono, I.J. Polmear, S.P. Ringer, The effects of a trace addition of silver upon elevated temperature ageing of an Al-Zn-Mg alloy. Micron **32** (8), 741-747 (2001).
DOI: https://doi.org/10.1016/S0968-4328(00)00081-0

[11] X.B. Yang, J.H. Chen, J.Z. Liu, F. Qin, J. Xie, C.L. Wu, A high-strength AlZnMg alloy hardened by the T-phase precipitates. J. Alloys Compd. **610**, 69-73 (2014).
DOI: https://doi.org/10.1016/j.jallcom.2014.04.185

[12] S. Onaka, Simple equations giving shapes of various convex polyhedra: the regular polyhedra and polyhedra composed of crystallographically low-index planes. Phil. Mag. Let. **86** (3), 175-183 (2006).
DOI: https://doi.org/10.1080/09500830600603050

[13] X. Zhang, Z. Han, L. Xu, H. Ni, X. Hu, H. Zhou et al., Evolution of precipitate and precipitate/matrix interface in Al-Zn-Mg-Cu (-Ag) alloys. J. of Mat. Sci. & Tech. **138**, 157-170 (2023).
DOI: https://doi.org/10.1016/j.jmst.2022.07.049

[14] W.V. Vaidya, Modification of the precipitate interface under irradiation and its effect on the stability of precipitates. J. of Nuc. Mat. **83** (1), 223-230 (1979).
DOI: https://doi.org/10.1016/0022-3115(79)90608-1

[15] Q. Lu, J. Wang, H. Li, S. Jin, G. Sha, J. Lu, Y. Du, Synergy of multiple precipitate/matrix interface structures for a heat resistant high-strength Al alloy. Nat. Comm. **14** (1), 2959 (2023).
DOI: https://doi.org/10.1038/s41467-023-38730-z

[16] K. Zhao, G. Han, T. Gao, H. Yang, Z. Qian, K. Hu, X. Liu, Interface precipitation and corrosion mechanisms in a model Al–Zn–Mg–Cu alloy strengthened by TiC particles. Corro. Sci. **206**, 110533 (2022).
DOI: https://doi.org/10.1016/j.corsci.2022.110533

[17] M. Yamaguchi, T. Tsuru, K.I. Ebihara, M. Itakura, K. Matsuda, K. Shimizu, H. Toda, Hydrogen Trapping in Mg_2Si and Al7FeCu2 Intermetallic Compounds in Aluminum Alloy: First-Principles Calculations. Mat. Trans. **61** (10), 1907-1911 (2020).
DOI: https://doi.org/10.2320/matertrans.MT-M2020201

[18] C. Cao, D. Zhang, Z. He, et al., Enhanced and accelerated age hardening response of Al-5.2Mg-0.45Cu (wt%) alloy with Zn addition. Mater. Sci. Eng. **A 666**, 34-42 (2016).
DOI: https://doi.org/10.1016/j.msea.2016.04.022

[19] G. Sha, A. Cerezo, Characterization of precipitates in an aged 7xxx series Al alloy. Surf. Interface Anal. **36** (5-6), 564-568 (2004).
DOI: https://doi.org/10.1002/sia.1702

[20] A.K. Mukhopadhyay, et al., Transactions of The Indian Institute of Metals **62**, 2, 113-122 (April 2009).
DOI: https://doi.org/10.1007/s12666-009-0015-z

[21] M. Bernole, R. Graf, Influence du zinc sur la decomposition de la solution solide sursaturee Al-Zn-Mg. Mem. Sci. Rev. Met. **69**, 123-133 (1972).

[22] A. Ahmed, S. Lee, T. Tsuchiya, K. Matsuda, et al., Microstructure Observation of T-phase in Al-Zn-Mg Alloy with low Zn/Mg ratio. J. of Al. and Comp. (2024).
DOI: https://doi.org/10.1016/j.jallcom.2024.177781

[23] C. Cao, Enhanced and accelerated age hardening response of Al-5.2Mg-0.45Cu (wt%) alloy with Zn addition. Materials Science & Engineering A **666**, 34-42 (2016).
DOI: https://doi.org/10.1016/j.msea.2016.04.022

[24] T. Tsuchiya, K. Uttarasak, S. Lee, A. Ahmed, et al., Existence of hexagonal tabular β-phase in Al-Mg-Si alloys containing noble metal elements. Mat. Tod. Comm. **35**,106198 (2023).
DOI: https://doi.org/10.1016/j.mtcomm.2023.106198